

REPORT DOCUMENTATION PAGE

Form Approved OMB NO. 0704-0188

The public reporting burden for this collection of information is estimated to average 1 hour per response, including the time for reviewing instructions, searching existing data sources, gathering and maintaining the data needed, and completing and reviewing the collection of information. Send comments regarding this burden estimate or any other aspect of this collection of information, including suggestions for reducing this burden, to Washington Headquarters Services, Directorate for Information Operations and Reports, 1215 Jefferson Davis Highway, Suite 1204, Arlington VA, 22202-4302. Respondents should be aware that notwithstanding any other provision of law, no person shall be subject to any penalty for failing to comply with a collection of information if it does not display a currently valid OMB control number.

PLEASE DO NOT RETURN YOUR FORM TO THE ABOVE ADDRESS.

1. REPORT DATE (DD-MM-YYYY) 16-10-2013	2. REPORT TYPE Final Report	3. DATES COVERED (From - To) 1-Oct-2012 - 30-Jun-2013		
4. TITLE AND SUBTITLE ARO STIR: DEFINING PEPTIDE NANOSTRUCTURES BY ENGINEERING ASSEMBLY INTERFACES		5a. CONTRACT NUMBER W911NF-12-1-0258		
		5b. GRANT NUMBER		
		5c. PROGRAM ELEMENT NUMBER 611102		
6. AUTHORS Sameer Sathaye, Nandita Bhagwat, Darrin J. Pochan, Kristi L. Kiick		5d. PROJECT NUMBER		
		5e. TASK NUMBER		
		5f. WORK UNIT NUMBER		
7. PERFORMING ORGANIZATION NAMES AND ADDRESSES University of Delaware 210 Hullihen Hall Newark, DE		8. PERFORMING ORGANIZATION REPORT NUMBER		
9. SPONSORING/MONITORING AGENCY NAME(S) AND ADDRESS(ES) U.S. Army Research Office P.O. Box 12211 Research Triangle Park, NC 27709-2211		10. SPONSOR/MONITOR'S ACRONYM(S) ARO		
		11. SPONSOR/MONITOR'S REPORT NUMBER(S) 61661-LS-II.2		
12. DISTRIBUTION AVAILABILITY STATEMENT Approved for Public Release; Distribution Unlimited				
13. SUPPLEMENTARY NOTES The views, opinions and/or findings contained in this report are those of the author(s) and should not be construed as an official Department of the Army position, policy or decision, unless so designated by other documentation.				
14. ABSTRACT This short-term innovative research proposal was focused on the structural characterization of peptide-based, self-assembled nanostructures of specific dimensions that are controlled by the geometry and physicochemical properties of the assembly interface. Our objectives were to (i) explore solution conditions that allow the production of nanostructures of select structural properties, specifically via the use of gradient hydrophobic interfaces, and (ii) characterize the conformation, fibril formation, and network properties of these peptide-based				
15. SUBJECT TERMS peptide assembly, beta sheet, fibrillar networks, peptide hydrogels				
16. SECURITY CLASSIFICATION OF: a. REPORT UU		17. LIMITATION OF ABSTRACT b. ABSTRACT UU	15. NUMBER OF PAGES	19a. NAME OF RESPONSIBLE PERSON Kristi Kiick
		c. THIS PAGE UU		19b. TELEPHONE NUMBER 302-831-0201

Report Title

ARO STIR: DEFINING PEPTIDE NANOSTRUCTURES BY ENGINEERING ASSEMBLY INTERFACES

ABSTRACT

This short-term innovative research proposal was focused on the structural characterization of peptide-based, self-assembled nanostructures of specific dimensions that are controlled by the geometry and physicochemical properties of the assembly interface. Our objectives were to (i) explore solution conditions that allow the production of nanostructures of select structural properties, specifically via the use of gradient hydrophobic interfaces, and (ii) characterize the conformation, fibril formation, and network properties of these peptide-based materials via a suite of circular dichroic spectroscopy (CD), oscillatory rheology, microscopy (AFM, SEM, TEM), and scattering (SANS) methods.

We have successfully achieved the aims of this STIR project, and have clearly demonstrated that (i) beta-hairpin structures can be formed by peptides with gradient hydrophobic faces comprising non-natural amino acids, (ii) these peptides are competent for fibril formation, and (iii) fibril formation and branching (as indicated by resulting network mechanical properties) can be modulated by modifications of the gradient of the hydrophobic interface. Loose packing of the designed fibrils is indicated, on the basis of initial SANS analysis, suggesting opportunities to modify the fibril interface with a range of chemically and electronically diverse hydrophobic amino acids, which will provide new opportunities to make smart materials for in-situ sensing and device fabrication.

Enter List of papers submitted or published that acknowledge ARO support from the start of the project to the date of this printing. List the papers, including journal references, in the following categories:

(a) Papers published in peer-reviewed journals (N/A for none)

Received Paper

TOTAL:

Number of Papers published in peer-reviewed journals:

(b) Papers published in non-peer-reviewed journals (N/A for none)

Received Paper

TOTAL:

Number of Papers published in non peer-reviewed journals:

(c) Presentations

No presentations on just this work to date.

Number of Presentations: 0.00

Non Peer-Reviewed Conference Proceeding publications (other than abstracts):

Received Paper

TOTAL:

Number of Non Peer-Reviewed Conference Proceeding publications (other than abstracts):

Peer-Reviewed Conference Proceeding publications (other than abstracts):

Received Paper

TOTAL:

Number of Peer-Reviewed Conference Proceeding publications (other than abstracts):

(d) Manuscripts

Received Paper

10/16/2013 1.00 Sameer Sathaye, Nandita Bhagwat, Kristi L. Kiick, Darrin J. Pochan. DEFINING PEPTIDE NANOSTRUCTURES BY ENGINEERING ASSEMBLY INTERFACES, Manuscript in preparation (04 2014)

TOTAL: 1

Number of Manuscripts:

Books

TOTAL:**Patents Submitted****Patents Awarded****Awards**

None to report on this work alone.

Pochan and Kiick both recently inducted as Fellows in respective professional societies. Kiick awarded Academic Research Award by the Delaware Biosciences Association.

Graduate Students

<u>NAME</u>	<u>PERCENT SUPPORTED</u>	Discipline
Sameer Sathaye	0.50	
Nandita Bhagwat	0.33	
FTE Equivalent:	0.83	
Total Number:	2	

Names of Post Doctorates

<u>NAME</u>	<u>PERCENT SUPPORTED</u>
FTE Equivalent:	
Total Number:	

Names of Faculty Supported

<u>NAME</u>	<u>PERCENT SUPPORTED</u>	National Academy Member
Kristi Kiick	0.00	No
Darrin Pochan	0.00	No
FTE Equivalent:	0.00	
Total Number:	2	

Names of Under Graduate students supported

<u>NAME</u>	<u>PERCENT SUPPORTED</u>
FTE Equivalent:	
Total Number:	

Student Metrics

This section only applies to graduating undergraduates supported by this agreement in this reporting period

The number of undergraduates funded by this agreement who graduated during this period: 0.00

The number of undergraduates funded by this agreement who graduated during this period with a degree in science, mathematics, engineering, or technology fields:..... 0.00

The number of undergraduates funded by your agreement who graduated during this period and will continue to pursue a graduate or Ph.D. degree in science, mathematics, engineering, or technology fields:..... 0.00

Number of graduating undergraduates who achieved a 3.5 GPA to 4.0 (4.0 max scale):..... 0.00

Number of graduating undergraduates funded by a DoD funded Center of Excellence grant for Education, Research and Engineering:..... 0.00

The number of undergraduates funded by your agreement who graduated during this period and intend to work for the Department of Defense 0.00

The number of undergraduates funded by your agreement who graduated during this period and will receive scholarships or fellowships for further studies in science, mathematics, engineering or technology fields: 0.00

Names of Personnel receiving masters degrees

NAME

Total Number:

Names of personnel receiving PHDs

NAME

Total Number:

Names of other research staff

NAME

PERCENT SUPPORTED

FTE Equivalent:

Total Number:

Sub Contractors (DD882)

Inventions (DD882)

Scientific Progress

Please see attachment (and manuscript section for manuscript in preparation). Attachment here is the same manuscript draft.

Technology Transfer

ARO STIR: DEFINING PEPTIDE NANOSTRUCTURES BY ENGINEERING ASSEMBLY INTERFACES

Darrin J. Pochan and Kristi L. Kiick, Materials Science and Engineering and Delaware Biotechnology Institute, University of Delaware

Research Area 9, Life Sciences

Program 9.1, Biochemistry

Stephanie McElhinny (stephanie.mcelhinny@us.army.mil, (919) 549-4240)

PROJECT SYNOPSIS

This short-term innovative research proposal was focused on the structural characterization of peptide-based, self-assembled nanostructures of specific dimensions that are controlled by the geometry and physicochemical properties of the assembly interface. Our objectives were to (i) explore solution conditions that allow the production of nanostructures of select structural properties, specifically via the use of gradient hydrophobic interfaces, and (ii) characterize the conformation, fibril formation, and network properties of these peptide-based materials via a suite of circular dichroic spectroscopy (CD), oscillatory rheology, microscopy (AFM, SEM, TEM), and scattering (SANS) methods.

We have successfully achieved the aims of this STIR project, and have clearly demonstrated that (i) β -hairpin structures can be formed by peptides with gradient hydrophobic faces comprising non-natural amino acids, (ii) these peptides are competent for fibril formation, and (iii) fibril formation and branching (as indicated by resulting network mechanical properties) can be modulated by modifications of the gradient of the hydrophobic interface. In-situ TEM measurements are being completed, to determine the cross-sectional dimensions of the fibrils. The packing of the designed fibrils is suggested, on the basis of initial SANS analysis, to be loose, suggesting opportunities to modify the fibril interface with a range of chemically and electronically diverse hydrophobic amino acids.

The successful demonstration of our STIR objectives suggests that the programming of select chemical function into the cores of these fibrillar structures is possible, which has direct importance to remote sensing, in-situ reporting of material integrity, and/or integration of prosthetic devices with patient tissues. Such approaches could thus afford new opportunities in the production of Army-relevant materials across applications relevant to both the protection and healing of military personnel, and will be the basis of future proposed work.

RESULTS of SUPPORTED WORK (manuscript in preparation)

Introduction

Specific molecular recognition (SMR) between functional groups of polymers, proteins, and peptides has been widely used as a tool to develop smart materials of both natural and synthetic origin. Fundamentally, SMR interactions are at the heart of biologically important processes such as protein-protein interactions, self-assembly, protein ligand interactions, phospholipid interactions, and cation- π interactions.¹⁻⁶ The literature is replete with reports of various types of non-covalent specific molecular recognition interactions, which have been instrumental in developing materials such as molecularly imprinted polymers, dendrimers and hydrogel networks for various applications such as catalysis, biosensing, drug design, chemical separations, drug delivery, and tissue engineering. Shape-specific molecular recognition has been studied widely in proteins but not with an objective of functional materials development;⁷⁻¹⁰ peptide interfaces offer a particularly attractive approach for such development.

Types of β -hairpin peptides, previously investigated, hierarchically assemble into fibrillar networks in aqueous environments by means of hydrogen bonding and non-specific hydrophobic interactions between geometrically ‘flat’ valine faces of a pair of peptides.¹¹⁻¹⁴ The non-specific hydrophobic interactions have a significant influence on the fibrillar nanostructure and rheological properties of the resulting network. In this work, we discuss the effects of shape-specific hydrophobic interactions introduced via design of new peptides with hydrophobic faces resembling ‘wedge’ and ‘trough’ shapes, on the self-assembly and network formation by the new hairpins. The results are presented in comparison to networks formed by hairpins with a flat hydrophobic face.

MAX1 is a β -hairpin peptide with alternating hydrophobic valine and hydrophilic lysine residues, with a –V^DPPT- turn sequence in the middle. At neutral to low pH, due to repulsion between positively charged lysine side chains, MAX1 adopts random coil conformations in aqueous solution. Changing solution conditions by raising pH (~9), increasing ionic strength (~150mM), or elevating temperature, causes MAX1 to fold into the β -hairpin conformation, with triggering of consequent intermolecular assembly, owing to the deprotonation or screening of charged lysine residues. Each hairpin is stabilized by significant hydrogen bonding between the arms of the peptide as well as the conformation of the turn sequence that anchors the arms. Increasing temperature also promotes the hydrophobic interactions between the hydrophobic side chains of the valine residues and serves as another factor that affects folding and assembly.

Multiple interactions stabilize the fibrillar assembly and network formation of MAX1 peptides. These include the lateral intermolecular hydrogen bonding and hydrophobic interactions between folded hairpins, which define the axis of the growing fibrils. Facial hydrophobic interactions between the valine faces of two hairpins form the cross-section of a growing fibril. In addition, defects manifest by an incomplete burial of valine leaves an exposed valine face that results in formation of a branch point in the fibril growth, leading to nucleation of two daughter fibrils. In addition to fibrillar entanglement, these branch points act as points of fibrillar physical crosslinking leading to formation of a self-standing hydrogel network.¹⁵ It is the lack of shape specificity in the facial hydrophobic interactions between peptides that at least partially contributes to these defects and new branch/crosslink points.^{11,12,16-18} Thus, the facial and lateral

hydrophobic interactions have a profound influence on the self-assembly kinetics, fibrillar nanostructure and network rheological properties of the MAX1 peptides.

In this report, we discuss the effects of introducing shape specificity to the hydrophobic face of newly designed β -hairpin peptides based on the original MAX1 sequence. Three pairs of peptides have been designed and studied (Figure 1). These pairs of peptides – LP1-KP1, LP2-KP2 and LP3-KP3 – have gradients in their local hydrophobic shape as shown in Figure 1, resulting either in a ‘wedge’ profile (LP1, LP2 and LP3) or a ‘trough’ profile (KP1, KP2 and KP3). These variations in shape may provide opportunities to control the specific orientations of β -hairpin assembly, thus affecting the fibrillar nanostructure and rheological properties of the networks.

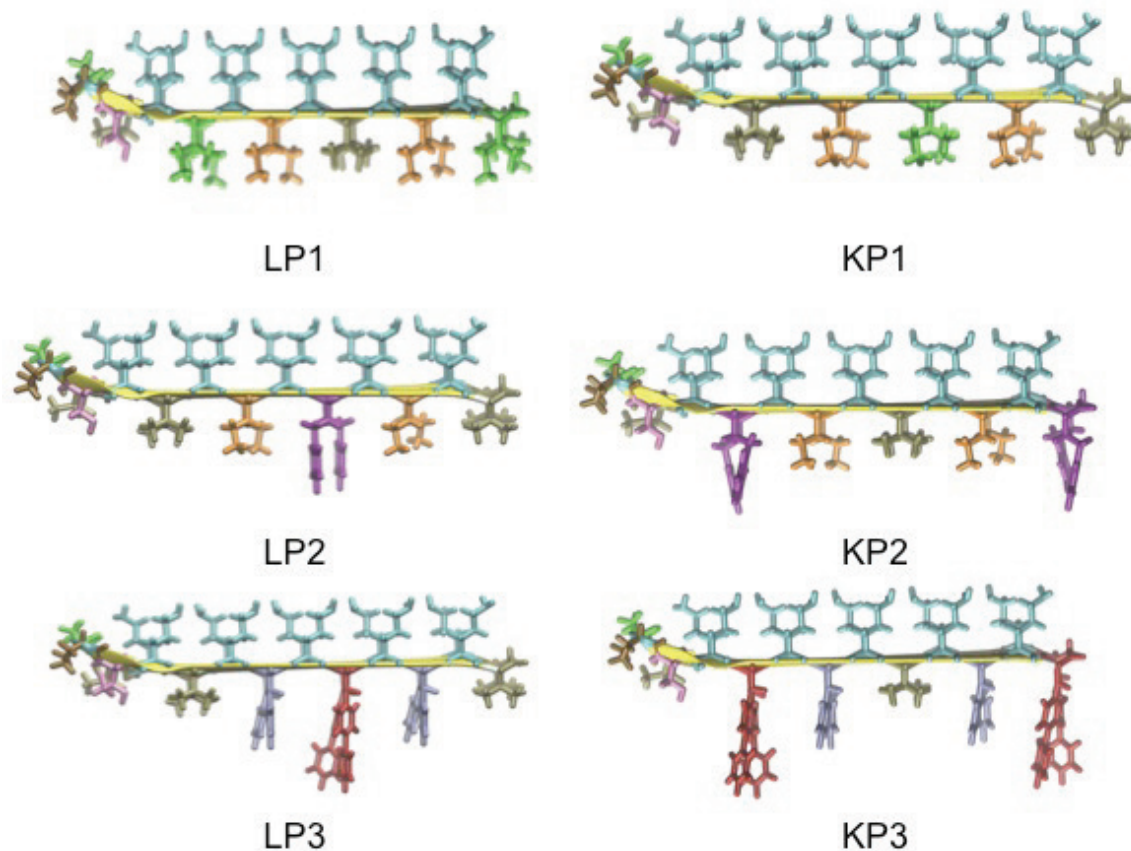


Figure 1. Schematic representations of the peptides LP1, KP1, LP2, KP2, LP3, KP3 when folded into a β -hairpin conformation.

Specifically, the peptides contain 24 residues (longer than the original MAX1 peptides consisting of 20 residues), with the valine groups selectively substituted with residues with sterically larger or smaller hydrophobic side chains (on both arms of the hairpins) flanking the $-V^D$ PPT- turn sequence. In order to preserve the similarity of the overall hydrophobic character of, and thus assembly conditions for, the designed peptides to those of MAX1, the lysine residues on the hydrophilic face of MAX1 were replaced by slightly shorter (and less hydrophobic) ornithine residues in the designed peptides. The shape-specific interactions in the hydrophobic core of the LP-KP fibrils should permit the formation of unbranched fibrils, in contrast to the branched fibrils of MAX1, and so

should form fibrillar percolated networks only by fibril entanglement. We report here the assembly of the newly designed peptides and their blends, the assembled fibril nanostructure and ultimate hydrogel network structure, characterized via a combination of techniques such as circular dichroic spectroscopy (CD), transmission electron microscopy (TEM), oscillatory rheological measurements, and small angle neutron scattering (SANS).

Experimental Section

Peptide Synthesis

The peptides LP1, KP1, LP2, KP2, LP3 and KP3 and MAX1 were purchased from New England Peptide, LLC (Gardener, MA, USA). All peptides were prepared using Fmoc-based solid-phase peptide synthesis as described elsewhere.

Peptide Assembly and Hydrogel Preparation

A 1 mg aqueous solution of a single peptide (or 1:1 blend by weight of pairs of peptides LP1:KP1, LP2:KP2, LP3:KP3), in 100 μ L of deionized chilled water (5°C) was prepared to yield a 1% (w/v) aqueous solution. An equal amount of chilled (5°C) buffer solution was added to the aqueous solution to give buffered solutions of the peptide. The buffer solution used depends upon the hydrophobicity of peptide or pair of peptides to be assembled. Peptide assembly was then triggered by raising the temperature of the solution to 30°C. All peptides assemble into hydrogels of various mechanical strengths, depending upon their sequence. The buffer solutions used were (i) pH 9 (250 mM boric acid, 20 mM NaCl) for LP1, KP1 and LP1:KP1; (ii) pH 7 (100 mM BTP, 300 mM NaCl) for LP2, KP2 and LP2:KP2; and (iii) pH 7 (100 mM BTP, 100 mM NaCl) for LP3, KP3 and LP3:KP3. Mixing of these buffers with the aqueous solutions of peptide(s) ultimately yielded solutions of (i) pH 9 (125 mM boric acid, 10 mM NaCl), (ii) pH 7 (50 mM BTP, 150 mM NaCl), and (iii) pH 7 (50 mM BTP, 50 mM NaCl) for the groups of peptides.

Circular Dichroic Spectroscopy

CD spectra were collected using a Jasco J-810 spectropolarimeter (Jasco Inc. Easton, MD, USA). 150 μ M solutions of peptides (total final concentration) were prepared by adding equal volumes of chilled (5°C) buffer solution to 300 μ M de-ionized peptide solution depending upon the peptide (or peptide mixture) used, as stated above. The random coil to β -hairpin folding transition temperatures were determined by scanning temperatures from 5°C to 80°C keeping the wavelength of incident radiation fixed at 218nm, the signature wavelength at which a significant drop in mean residual ellipticity indicates the formation of β -sheet secondary structure. Mean residue ellipticity $[\theta]$ was calculated from the equation, $[\theta] = \theta_{\text{obs}} / (10 \times 1 \times c \times n)$ where θ_{obs} is the measured ellipticity (millidegrees), 1 is the path length of the cell (cm), c is the peptide concentration (M), and n is the number of residues on the peptide sequence. The pathlength of the cuvette used for CD experiments was 1 mm for the samples LP1, KP1, 1:1 (w/w) LP1:KP1, LP2, KP2 and 1:1 (w/w) LP2:KP2. The path length of the cuvette was 0.5 mm for the samples LP3, KP3, and 1:1 (w/w) LP3:KP3. Temperature scans were

performed with 2 °C increments and 5 min equilibration time at each temperature.

Oscillatory Rheology

Oscillatory rheology measurements were performed on an ARG2 rheometer (TA Instruments, New Castle, DE, USA) using a 20mm diameter stainless steel parallel plate geometry. Buffered peptide solutions 1% (w/v; single peptide) or 2% (w/v; mixture of peptides, 1wt% of each peptide) were prepared in ice-chilled solutions by adding 100 μ L of chilled (5° C) buffer to 100 μ L of 2% or 4% (w/v) of peptide solution in chilled (5° C) deionized water. The peptide hydrogels used for rheological experiments were LP1, LP2, LP3 at 1% (w/v) effective concentration and 1:1 mixtures (by weight) of LP1:KP1, LP2:KP2 and LP3:KP3 at 2% (w/v) effective concentration (i.e. 1% (w/v) of each component in the solution). The peptide mixtures were prepared at 2wt% in order to assess the impact of a stoichiometric addition of a KP peptide to an LP peptide of known mechanical properties. The chilled (5° C) buffered peptide solution was quickly transferred to the Peltier plate of the ARG2 rheometer equilibrated at 5°C, and the upper plate was lowered to a gap height of 500 μ m. The upper plate and the Peltier plate were equilibrated to 30°C prior to carrying out the rheological experiments. Oscillatory time sweep measurement steps were carried out for each solution, for 90 minutes before and 90 minutes after subjecting the hydrogel networks to a steady state shear of 1000/s for 120 sec. Throughout the measurements the oscillatory frequency was maintained at 6 rad/s and oscillatory strain at 1%. The gap height was maintained at 500 μ m for both the experiments.

Small Angle Neutron Scattering (SANS)

SANS experiments were performed on the 30 m instrument (NG-3) at the NIST Center for Neutron Research (NCNR), National Institute of Standards and Technology (NIST), Gaithersburg, MD. All gel samples (a) LP1, KP1, LP1:KP1 1:1 (w/w) (pH 9 (125 mM boric acid, 10 mM NaCl)), (b) LP2, KP2, LP2:KP2 1:1 (w/w) (pH 7 (50 mM BTP, 150 mM NaCl)), and (c) LP3, KP3, LP3:KP3 1:1 (w/w) (pH 7 (50 mM BTP, 50 mM NaCl)) were prepared at a 1% (w/v) effective concentration by mixing the peptide and buffer solutions (where both were prepared in D2O to enable adequate contrast between the hydrogen-rich gel matrix and the deuterated solvent). Solutions pre-equilibrated at 5° C were mixed in a vial and transferred immediately to titanium sample cells with 25 mm diameter quartz windows and a 1 mm path length. All samples were incubated at room temperature for 3 hours prior to scattering measurements. A monochromated neutron beam ($\lambda = 6 \text{ \AA}$) with a wavelength spread ($\delta I/I$) of 0.12 was incident on the sample. The scattered neutrons were captured on a 64 cm X 64 cm 2D detector. Varying sample-to-detector distances of 1.33, 4.5 and 13.17 m were used to the study of the scattering wavevector q in the range $0.004 < q (\text{\AA}^{-1}) < 0.4$, defined by $q = (4\pi/\lambda) \sin (\theta/2)$, where λ is the neutron wavelength and θ is the scattering angle. Raw data were corrected for background electronic noise and radiation, detector inhomogeneity and sensitivity, and empty cell scattering. Intensities were normalized to an absolute scale relative to main beam transmission measurements through the sample and were reduced according to published protocol.¹⁹ The error bars of the data points for all SANS plots are within the limits of the symbols.

Transmission Electron Microscopy (TEM)

Transmission electron microscopy was conducted on a 120kV Tecnai-12 Electron Microscope (FEI Company, Hillsboro, OR, USA). Peptide assembly of each peptide and the blends of pairs was triggered as described above, at 0.5% (w/v) concentration. 10 μ L of assembled peptide hydrogel sample was diluted to a concentration of 0.1% (w/v), and a drop was placed on a 300 mesh copper-coated grid (Electron Microscopy Sciences, Hatfield, PA, USA) held by a pair of tweezers. Excess fluid was blotted off with a filter paper, and 3 μ L of a 1 % (w/v) of uranyl acetate solution in water was immediately placed on the grid and blotted off after 40 sec. The grid was left to dry for an hour and then used for imaging.

Results and Discussion

Circular Dichroic Spectroscopy

The new peptides are designed to have an increasingly steep gradient of the wedge shape (in the order LP1, LP2 and LP3) and trough shape (in the order KP1, KP2 and KP3) as shown in Figure 1. Thus, LP2 and KP2 were designed to show intermediate hydrophobic shape specificity to that of LP1, KP1 and LP3, KP3 peptides. Circular dichroic spectroscopy experiments were performed to investigate the β -hairpin formation of the new peptides and to determine suitable solution conditions for potential self-assembly of the peptides. The mean residual ellipticity (MRE, deg $\text{cm}^2/\text{decimole}$) at 218 nm was plotted as a function of temperature ($^{\circ}\text{C}$) for each sample and a transition temperature from random coil to β -sheet conformation was determined for the sample under the given solution conditions. The MAX1 peptide (150 μM) folds from a random coil conformation to a β -sheet structure at 30 $^{\circ}\text{C}$ in a pH 9 buffer (125 mM boric acid, 10 mM NaCl) (Figure 2a); the CD spectrum represents contributions from individual β -hairpins of MAX1 as well as the assembled β -sheet fibrils. As shown in the figure, the LP1 and KP1 peptides (Figure 2b) undergo a conformational change from random coil conformation to β -sheet structure at the same solution conditions as MAX1 (pH 9, 125 mM boric acid, 10 mM NaCl), but at lower temperatures (15 $^{\circ}\text{C}$) as compared to MAX1 (30 $^{\circ}\text{C}$) (Figure 2b), owing to their slightly higher overall hydrophobic nature versus that of MAX1. As the LP2 and KP2 peptides (Figure 2c) are significantly more hydrophobic than MAX1, they undergo a conformational change from a random coil conformation to a β -sheet structure at a weaker solution stimulus (pH 7, 50 mM BTP, 150 mM NaCl) than MAX1 and LP1. By the virtue of having the steepest gradient of the wedge and trough shape and thus containing the amino acids with the largest side chain volume, LP3 and KP3 peptides are most hydrophobic in the series of the newly designed peptides. LP3 (Figure 2d) thus undergoes a conformational change from a random coil conformation to a β -sheet structure at the weakest solution conditions (pH 7, 50 mM BTP, 50 mM NaCl). The data show distinct folding profiles for the mixtures of peptides versus those observed for the LP or KP peptides alone, suggesting the formation of mixed fibril species in the LP:KP mixtures. Although the solution conditions and temperatures necessary to trigger β -hairpin formation are slightly different for the different peptides, the data indicate that they all ultimately form β -sheet structures under easily probed experimental conditions and that the fibril and network structures of the various peptides and peptide pairs can thus be compared.

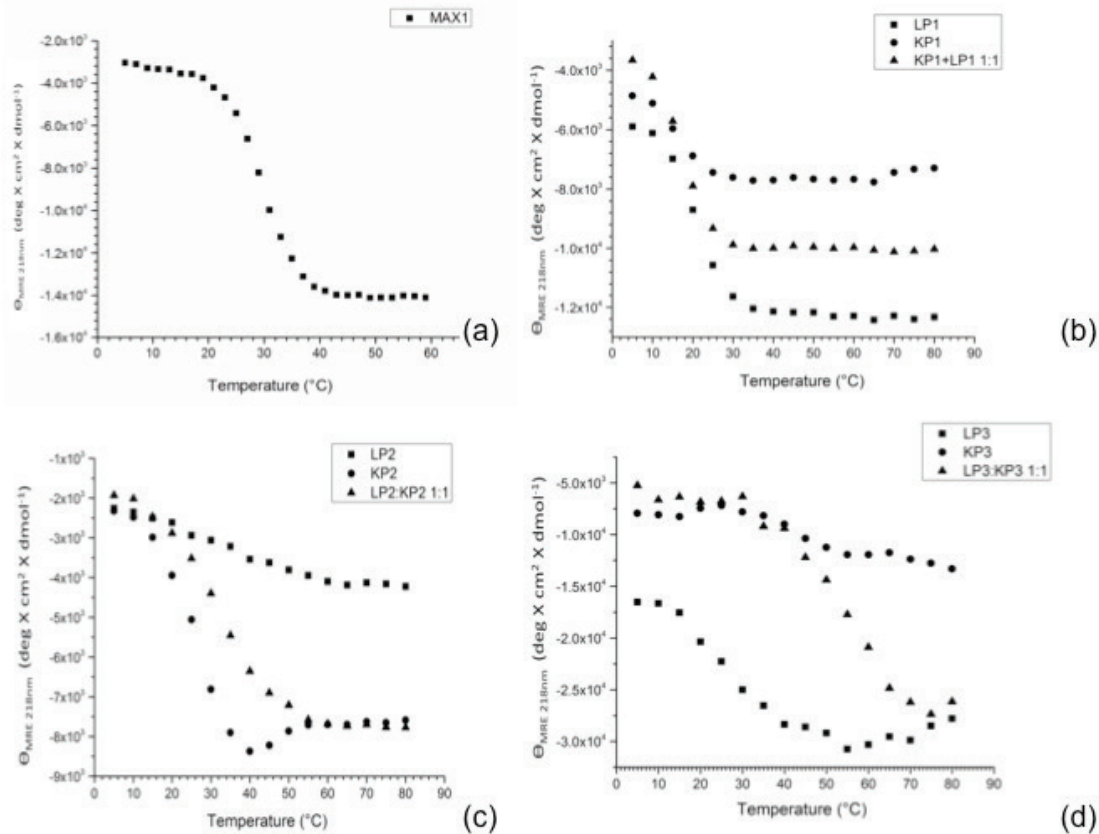


Figure 2. Circular dichroic spectroscopy data (mean residue ellipticity in $\text{deg} \cdot \text{cm}^2/\text{decimole}$ at 218 nm vs. temperature, °C) showing the different temperatures of the folding transition from random coil to β -sheet secondary conformation at 150 μM concentration for (a) MAX1 at pH 9 (125 mM boric acid, 10 mM NaCl); (b) LP1, KP1, LP1:KP1 1:1; all at pH 9 (125 mM boric acid, 10 mM NaCl); (c) LP2, KP2, LP2:KP2 1:1 all at pH 7 (50 mM BTP, 150 mM NaCl); and (d) LP3, KP3, LP3:KP3 1:1 all pH 7 (50 mM BTP, 50 mM NaCl). Solid squares indicate LP peptides, solid circles KP peptides and solid triangles 1:1 LP:KP blends.

Oscillatory Rheology

Solid MAX1 hydrogels exhibit a unique property of undergoing shear thinning and flow under a large amplitude applied shear stress, but immediately recovering into solid gels on cessation of shear. An earlier study by Yan et al.,¹⁸ which explored the hydrogel behavior during and after flow, indicated the gel networks fracture into domains much larger than the length scale of individual fibrils in order to flow. The network morphology within gel domains during flow was structurally identical to the parent

network at rest; the peptide fibrils displayed the same cross-section, the same physical crosslinking points of fibrillar entanglement and branching, and the same porosity. On cessation of shear, the gel domains immediately re-percolate to form a bulk, hydrogel network (Figure 3a). This shear-thinning and rehealing behavior of MAX1 would not exist if the network disintegrated into individual fibrils during flow since there would be no immediate mechanism for the fibrils to recrosslink and percolate into a bulk network. If the fibril branching in MAX1 is responsible for the observed shear thinning an immediate gel reformation behavior, then ridding the system of most fibril branching should significantly affect the hydrogel flow properties.

The hydrophobic shape-specific interactions in the LP and KP peptides are anticipated to eliminate fibril branching in the networks and thus produce networks which display shear thinning behavior but not rehealing characteristics as shown by MAX1. Inspection of Figure 3b illustrates that the LP1 peptides form hydrogels, which show shear thinning behavior as well as rehealing behavior, suggesting that the LP1 peptide alone forms branching fibrils. When an equal amount of KP1 is introduced to a 1% (w/v) of LP1, a network of higher stiffness is formed, likely attributable to the overall higher concentration (2% (w/v)) of peptide in the LP1:KP1 hydrogel, as compared to 1% (w/v) in case of pure LP1). The rehealing of these networks suggests that the hydrophobic interactions between the LP1 and KP1 are not specific enough to eliminate branching.

When the same rheometric experiment is performed on a 1% (w/v) LP2 hydrogel (Figure 3c), shear thinning as well as partial rehealing behavior is observed. Interestingly, when an equal amount to KP2 is introduced to a 1% (w/v) solution of LP2 (leading to an overall 2% (w/v) hydrogel), the observed stiffness of the network *decreases*. This suggests an elimination of branching, leading to weaker hydrogels, and indicates that some hydrophobic shape-specific interactions may be occurring in the LP2:KP2 1:1 mixture. Most importantly, the LP2:KP2 hydrogel shear thins but fails to recover to even 10% of the original storage modulus (G') of the original network. This lack of rehealing is indicative of significant elimination of branching in the networks from the blended peptides, providing direct proof of shape specificity at work.

Both shear thinning and rehealing behavior were observed when LP3 (1% (w/v)) and LP3:KP3 (2% (w/v)) peptide hydrogels were studied (Figure 3d), and a significant increase in mechanical strength for the LP3:KP3 hydrogels (vs. the LP3 hydrogels) was observed. The rehealing and reinforcement observed in the LP3:KP3 hydrogels is almost certain to arise from branch points, based on the detailed analysis of the behavior and structure of MAX1 hydrogels. Although the LP3 and KP3 peptides might be expected to have the greatest shape-specificity of the peptide pairs owing to the steep gradient of their hydrophobic faces, the rheology experiments suggest that the greater hydrophobicity of these interfaces leads to defect-induced branching. Thus, taken together, the rheological characterization of the hydrogels suggests that an optimum in hydrophobicity and gradient of wedge and trough shape is necessary for shape-specific hydrophobic interactions, and in these studies, is exhibited by only the pair LP2-KP2.

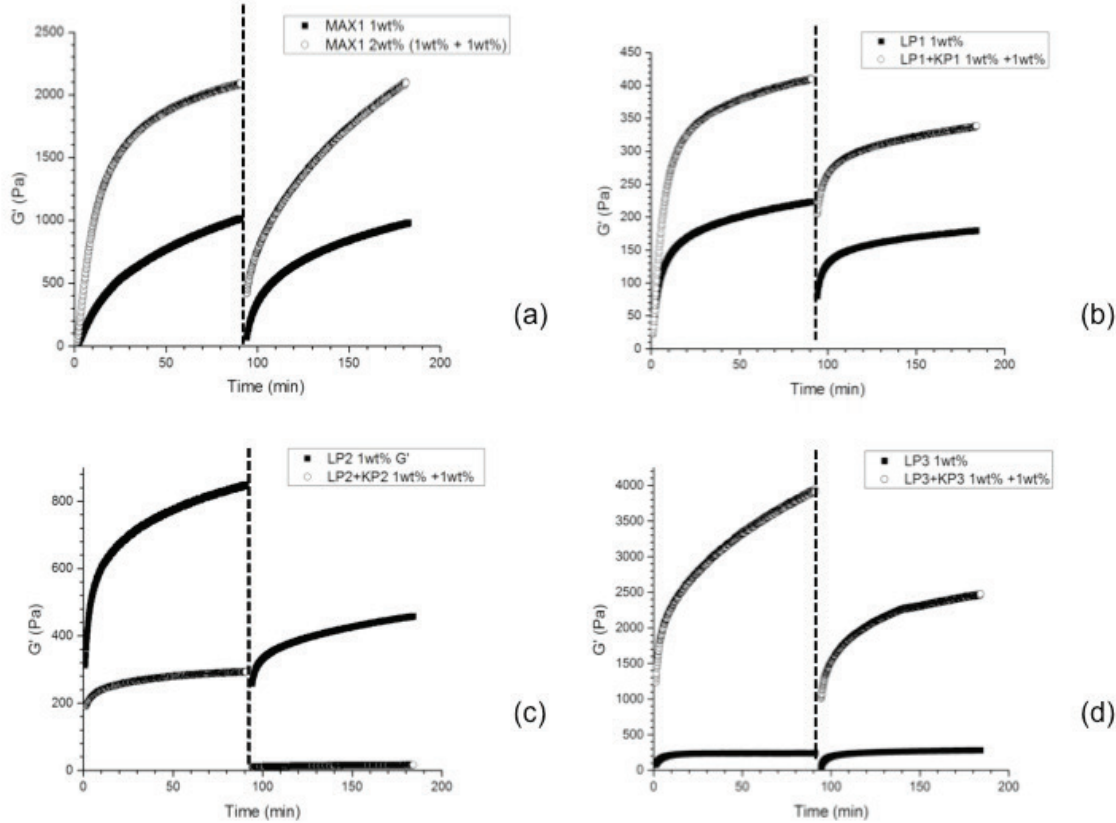


Figure 3. Oscillatory rheology time-sweep measurements before and after application of steady state shear (1000/s for 120 sec, indicated by dotted line) on (a) 1% and 2% (w/v) MAX1 at pH 9 (125 mM boric acid, 10 mM NaCl); (b) 1% LP1 and 1% (w/v) LP1+ 1% (w/v) KP1 at pH 9 (125 mM boric acid, 10 mM NaCl); (c) 1% LP2 and 1% (w/v) LP2+ 1% (w/v) KP2 at pH 7 (50 mM BTP, 150 mM NaCl); and (d) 1% LP3 and 1% (w/v) LP3+ 1% (w/v) KP3 at pH 7 (50 mM BTP, 50 mM NaCl).

Small Angle Neutron Scattering (SANS)

MAX1 forms self-assembled fibrils of a uniform \sim 3nm thickness (Figure 4a). When $I(q)$ v/s q data obtained from SANS measurements was fit to a cylindrical form factor in the q range of data on MAX1 samples, MAX1 fibrils fit very well to a cylindrical form factor. Also, as shown in Table 1, the slope ‘ n ’ of the $\log(I)$ vs. $\log(q)$ in the $(0.02 < q < 0.08)$ range for MAX1 is ~ 1 , which indicates rod-like or cylindrical assembled structures in the size range of 10-50 nm. Additionally, the slope ‘ m ’ of the $\log(I)$ vs. $\log(q)$ in the $(0.1 < q < 0.25)$ q - range (an individual fibrillar level) is ~ -4 , which indicates a smooth surface for each individual fibril. These data reinforce a uniformly packed cylindrical self-assembled structure for MAX1 that is also confirmed by TEM. Fitting of SANS data shown from LP1, LP2 and LP3 to a cylindrical form factor indicates that LP1, LP2 and

LP3 form cylindrical self-assembled structures (Figure 4b-d). While the data indicate that KP1, KP2, KP3 and the blends LP1:KP1, LP2:KP2 and LP3:KP3 all form self-assembled structures, an exact morphology determination of these structures is underway by means of in-situ electron microscopy and additional SANS analysis. The slopes of the log (I) vs. log (q) plot at the high q regime ($0.1 < q < 0.25$) (Table 1), for all of the LP and KP peptide samples, indicates a very rough surface at the individual fibrillar level, suggesting a lack of uniform packing as compared to a tightly packed fibrillar structure of MAX1. Thus, from the SANS data it can be inferred that assembled nanostructures from LP1, KP1, LP2, KP2, LP3, KP3 and their 1:1 mixtures demonstrate a much more loosely packed structure as compared to MAX1, as would be expected based on the more hydrophobic nature of their hydrophobic faces.

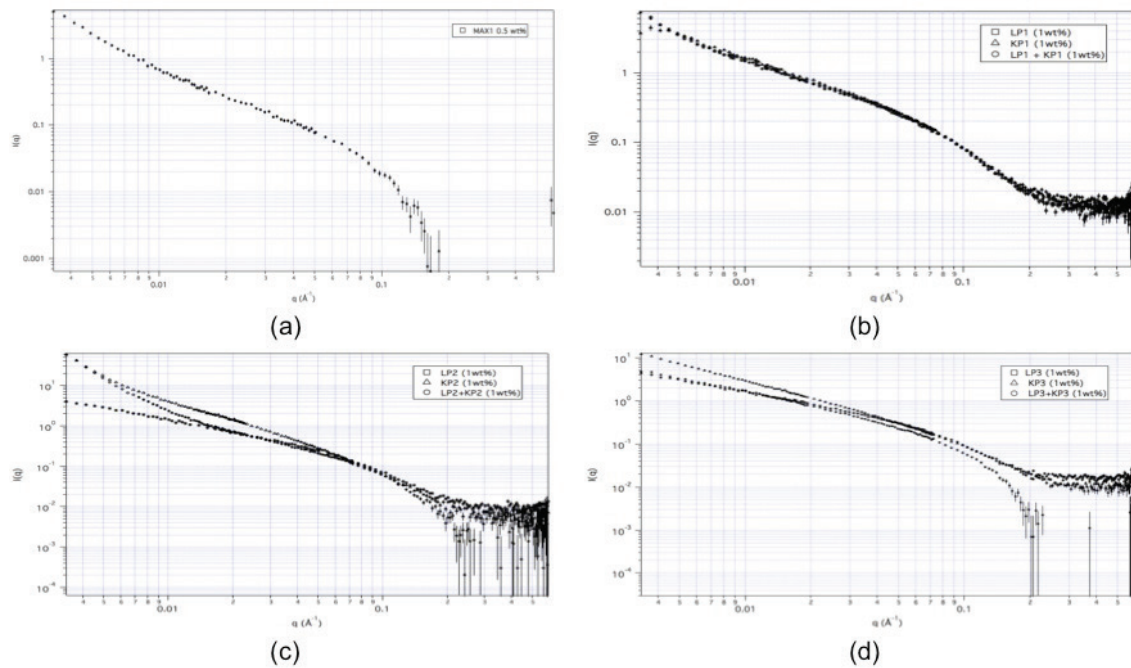


Figure 4. I (q) vs. q data from SANS measurements on (a) MAX1; (b) LP1, KP1, LP1:KP1 1:1; all at pH 7 (50 mM BTP, 150 mM NaCl); (c) LP2, KP2, LP2:KP2 1:1 all at pH 9 (125 mM boric acid, 10 mM NaCl); and (d) LP3, KP3, LP3:KP3 1:1 pH 7 (100 mM BTP, 100 mM NaCl). LP, KP concentrations were 1% (w/v) for individual peptides and 2% (w/v) for blends, indicating 1% (w/v) for each component. Hollow squares indicate LP peptides, hollow circles KP peptides and hollow triangles the 1:1 LP:KP blends.

Sample	Slope of log (I) v/s log (q) in intermediate q region 'n'	Slope of log (I) v/s log (q) in high q region 'm'
MAX1 0.5 wt%	-1.01 (0.007-0.06)	-4.10 (0.1-0.16)
LP1 1 wt%	-1.07 (0.005-0.06)	-2.09 (0.07-0.25)
KP1 1 wt%	-1.13 (0.005-0.06)	-2.01 (0.07-0.25)
1:1 LP1:KP1 1 wt%	-1.11 (0.005-0.06)	-2.01 (0.07-0.18)
LP2 1 wt%	-1.10 (0.007-0.06)	-2.18 (0.07-0.2)
KP2 1wt%	-1.66 (0.006-0.07)	-2.40 (0.07-0.25)
1:1 LP2:KP2 1 wt%	-1.40 (0.01-0.07)	-2.54 (0.07-0.2)
LP3 1 wt%	-1.09 (0.009-0.07)	-2.20 (0.08-0.2)
KP3 1 wt%	-1.43 (0.009-0.07)	-2.09 (0.07-0.25)
1:1 LP3:KP3 1 wt%	-1.24 (0.009-0.07)	-2.65 (0.07-0.18)

Table 1. Slopes of log (I) v/s log (q) for intermediate-q and high-q ranges. q-range specific to each sample listed in parenthesis.

Transmission Electron Microscopy (TEM)

TEM data obtained from all peptides LP1, KP1, LP2, KP2, LP3, KP3 and their blends as shown in Figure 5(a-i) shows aggregated fibrillar structures from each and every peptide. The sample preparation method for the obtained TEM data involves drying of a cast film of dilute hydrogel sample and is subject to artifacts, which result as a process of dilution and drying. The assembled fibrils from each peptide are expected to be ~4 nm in thickness and we suspect that it is due to the dilution process and drying artifacts that the assembled structures obtained from TEM shown here are much thicker (~25 nm) and do not accurately describe the actual structure of the assembled fibrils. Thus, further work on in-situ electron microscopy and its coherent correlation to data obtained from SANS is required and is underway.

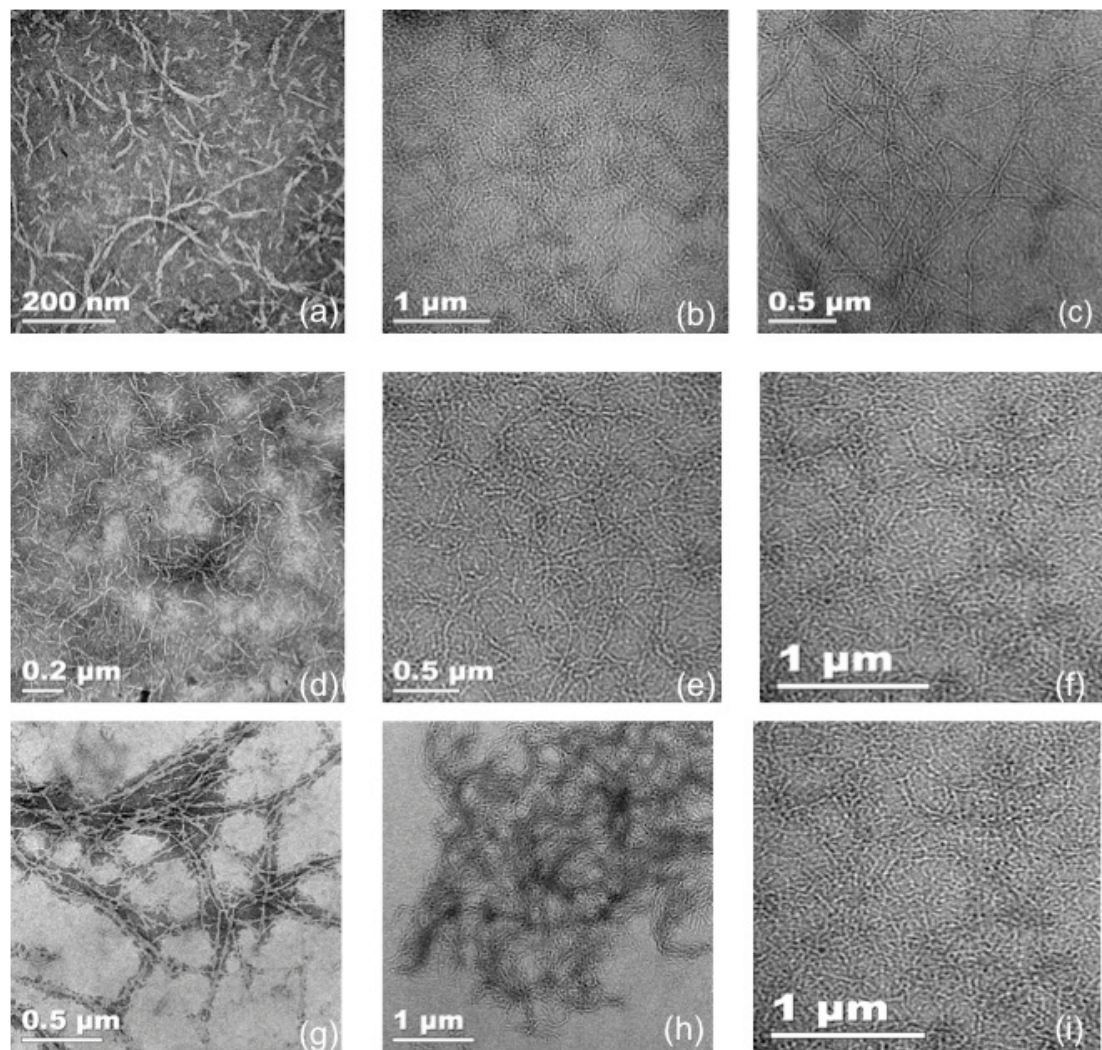


Figure 5. Transmission electron micrographs from (a) LP1 (b) KP1 (c) LP1:KP1 1:1, all at pH 9 (125 mM boric acid, 10 mM NaCl); (d) LP2 (e) KP2, (f) LP2:KP2, all at pH 7 (50 mM BTP, 150 mM NaCl); and (g) LP3 (h) KP3 (i) LP3:KP3 1:1, all at pH 7 (50 mM BTP, 50 mM NaCl) and stained with 1 % (w/v) uranyl acetate in deionized water.

Conclusions

We have successfully demonstrated that shape-specific hydrophobic interactions can be employed to manipulate the assembly and properties of self-assembling β -hairpin peptides. Each pair of peptides LP1-KP1, LP2-KP2 and LP3-KP3 (listed in order of an increasing gradient of local hydrophobic wedge- and trough-like shapes) underwent conformational transitions from random coil to β -sheet secondary structures in a manner similar to one another and to the parent sequence MAX1; minor changes in solution conditions were required for self-assembly. Rheological characterization of the hydrogels from the LP and KP peptides clearly suggests an optimum balance of hydrophobic interaction strength and gradient shape to minimize branching in networks comprising LP and KP peptides; the LP2:KP2 pair is suggested to have minimal branching owing to its lack of recovery after shear. TEM and SANS analysis indicates that fibrillar nanostructures were obtained from the LP peptides; the final self-assembled structures

adopted by the KP peptides and the LP:KP mixtures are being confirmed via further in-situ electron microscopy and SANS analysis. Initial analysis of SANS data indicates that loose packing in the assembled structures was observed in all the new peptides relative to the tight packing observed for MAX1, suggesting that these designed interfaces should have sufficient flexibility to accommodate hydrophobic side-chains of expanded chemical and electronic versatility. Thus, hydrophobic shape specificity was found to significantly influence the self assembled nanostructure and network rheological behavior in self assembling β -hairpin peptides.

References

- (1) Banwell, E. F.; Abelardo, E. S.; Adams, D. J.; Birchall, M. A.; Corrigan, A.; Donald, A. M.; Kirkland, M.; Serpell, L. C.; Butler, M. F.; Woolfson, D. N. *Nature Materials* **2009**, *8*, 596.
- (2) Shen, W.; Lammertink, R. G. H.; Sakata, J. K.; Kornfield, J. A.; Tirrell, D. A. *Macromolecules* **2005**, *38*, 3909.
- (3) Petka, W. A.; Harden, J. L.; McGrath, K. P.; Wirtz, D.; Tirrell, D. A. *Science* **1998**, *281*, 389.
- (4) Jing, P.; Rudra, J. S.; Herr, A. B.; Collier, J. H. *Biomacromolecules* **2008**, *9*, 2438.
- (5) Papapostolou, D.; Smith, A. M.; Atkins, E. D. T.; Oliver, S. J.; Ryadnov, M. G.; Serpell, L. C.; Woolfson, D. N. *Proceedings of the National Academy of Sciences of the United States of America* **2007**, *104*, 10853.
- (6) Foo, C.; Lee, J. S.; Mulyasasmita, W.; Parisi-Amon, A.; Heilshorn, S. C. *Proceedings of the National Academy of Sciences of the United States of America* **2009**, *106*, 22067.
- (7) Sacanna, S.; Irvine, W. T. M.; Chaikin, P. M.; Pine, D. J. *Nature* **2010**, *464*, 575.
- (8) Sprules, T.; Green, N.; Featherstone, M.; Gehring, K. *Journal of Biological Chemistry* **2003**, *278*, 1053.
- (9) Schwyzer, R. *Biopolymers* **1995**, *37*, 5.
- (10) Helm, C. A.; Knoll, W.; Israelachvili, J. N. *Proceedings of the National Academy of Sciences of the United States of America* **1991**, *88*, 8169.
- (11) Ozbas, B.; Kretsinger, J.; Rajagopal, K.; Schneider, J. P.; Pochan, D. J. *Macromolecules* **2004**, *37*, 7331.
- (12) Ozbas, B.; Rajagopal, K.; Haines-Butterick, L.; Schneider, J. P.; Pochan, D. J. *Journal of Physical Chemistry B* **2007**, *111*, 13901.
- (13) Pochan, D.; Schneider, J. *Biopolymers* **2003**, *71*, 317.
- (14) Rajagopal, K.; Lamm, M. S.; Haines-Butterick, L. A.; Pochan, D. J.; Schneider, J. P. *Biomacromolecules* **2009**, *10*, 2619.
- (15) Yucel, T.; Micklitsch, C. M.; Schneider, J. P.; Pochan, D. J. *Macromolecules* **2008**, *41*, 5763.
- (16) Schneider, J. P.; Pochan, D. J.; Ozbas, B.; Rajagopal, K.; Pakstis, L.; Kretsinger, J. *Journal of the American Chemical Society* **2002**, *124*, 15030.
- (17) Yan, C. Q.; Mackay, M. E.; Czynnemek, K.; Nagarkar, R. P.; Schneider, J. P.; Pochan, D. J. *Langmuir* **2012**, *28*, 6076.
- (18) Yan, C. Q.; Pochan, D. J. *Chemical Society Reviews* **2010**, *39*, 3528.
- (19) Kline, S. R. *Journal of Applied Crystallography* **2006**, *39*, 895.

